



APRIL 07 2025

Towards more accurate sound field verification using directional acoustic filtering

Emily Barosin  ; Kaustubha Raghukumar 



JASA Express Lett. 5, 046001 (2025)

<https://doi.org/10.1121/10.0036394>



Articles You May Be Interested In

Displaying bioacoustic directional information from sonobuoys using “azigrams”

J. Acoust. Soc. Am. (July 2019)

Automated two-dimensional localization of underwater acoustic transient impulses using vector sensor image processing (vector sensor localization)

J. Acoust. Soc. Am. (February 2021)

Automated two-dimensional localization of underwater acoustic transient impulses using vector sensor image processing

J. Acoust. Soc. Am. (October 2020)



ASA

Advance your science and career as a member of the
Acoustical Society of America

[LEARN MORE](#)



ASA
ACOUSTICAL SOCIETY
OF AMERICA

Towards more accurate sound field verification using directional acoustic filtering

Emily Barosin^{1,2}  and Kaustubha Raghukumar¹ 

¹Integral Consulting Inc., Santa Cruz, California 95060, USA

²Thayer School of Engineering, Dartmouth College, Hanover, New Hampshire 03755, USA

ebarosin@integral-corp.com, kraghukumar@integral-corp.com

Abstract: Attributing omnidirectional sound levels to a specific source in the ocean can be challenging when there are multiple competing sources of sound such as boats, or biological activity. Here, we present a method to directionally filter acoustic measurements based on vector measurements of acoustic pressure and particle velocity. The directional discrimination is applied to estimate sound energy from two marine energy sources: sound generated during the decommissioning of an oil platform and those from an operating tidal energy converter. The application of a directional mask leads to distinctly different spectra and some differences in energy, relative to the unmasked scenarios. © 2025 Author(s). All article content, except where otherwise noted, is licensed under a Creative Commons Attribution (CC BY) license (<https://creativecommons.org/licenses/by/4.0/>).

[Editor: David R Dall'Osto]

<https://doi.org/10.1121/10.0036394>

Received: 5 December 2024 **Accepted:** 26 March 2025 **Published Online:** 7 April 2025

1. Introduction

A key regulatory aspect for the permitting of anthropogenic noise-generating activities is sound source verification (SSV).^{1,2} This effort typically involves field measurements of underwater sound around noise-generating activities such as pile driving for offshore wind, with the goal of validating prior model predictions whose results may have been used in permit applications to agencies such as the Bureau of Ocean Energy Management or the National Marine Fisheries Service. SSV is typically performed using omnidirectional hydrophones deployed at various distances from a source whose acoustic output was first modeled using best guesses for source levels. However, measurements of sound in the vicinity of a source can reflect contributions from the source of interest in addition to contributions from ambient sources like waves, precipitation, animals, and shipping traffic, making it difficult to unambiguously identify and quantify sound attributable to a single source.

The use of directional acoustic sensing, such as vector sensors or tetrahedral arrays, can provide two- or three-dimensional bearing estimates to sources of sound.³ The parsing of acoustic data by frequency and direction (i.e., “azigrams”^{4,5}) can be a powerful tool for SSV. An azigram is a method of organizing and visualizing directional information of acoustic data across time and frequency. In essence, it is a spectrogram where the color of a coordinate is determined by the dominant directionality of active intensity.⁴ Here, we demonstrate the utility of using azigrams calculated acoustic vector sensor data as directional filters to estimate sound pressure levels from specific, known sources in the water column.

2. Experimental data and analysis

Data are gathered on a three-element, three-dimensional vector sensor array.⁶ The NoiseSpotter[®] (www.noisespotter.com) is equipped with three-vector sensors where each vector sensor measures both acoustic pressure and three-dimensional (3D) acoustic particle velocity in the 10 Hz–3 kHz frequency range. Sensors are mounted on three vertical poles arranged as a triangle and spaced by 1 m horizontally and 25 cm vertically, with the lowest sensor located 16 cm above the seafloor. While the sensors are located too close together to allow for beamforming, the proximity can allow for coherent averaging of time series to help isolate low signal-to-noise ratio signals. In this paper, however, only a single vector sensor is used since data from the other sensors in the data sets studied were found to be contaminated by flow and electronic noise.

The directional filtering method is applied to two data sets: (1) data collected to evaluate noise generated during oil platform decommissioning activities, such as the mechanical cutting of conductor pipes,^{7,8} and (2) data collected during the operation of a 3-foot by 4-foot vertical axis tidal energy turbine.⁹ For both data sets, a long-term spectral average (LTSA)¹⁰ is first computed on the acoustic pressure data to evaluate varying frequency contributions with time. An LTSA is essentially a spectrogram over long time periods where successive spectra are calculated and averaged over short time periods to provide a time series of the spectra. The LTSA is computed using 1024-point fast Fourier transforms (FFTs), Hanning windowed with no overlap between windows, and averaged over successive 10-s periods that result in a 10-s data resolution. Azigrams are also calculated using the same frequency resolution and temporal averaging as the LTSA.

Directional filtering is first applied to acoustic data collected close to *Platform Hermosa* near Santa Barbara, CA, during the mechanical cutting of its conductor pipes prior to the decommissioning of the oil platform. The NoiseSpotter was deployed 100 m from the oil platform at a bearing of 44° at 33.454°N, 120.648°W, in 189 m deep water on March 31, 2021, at 1800 Pacific Daylight Time. The system recorded continuously through April 8, 2021, and was recovered on April 21, 2021. The LTSA for the data collection period [Fig. 1(a)] shows broadband streaks of high intensity that are associated with periods of conductor cutting activity. The dominant directionality of this intensity is between 40 and 60 degrees from true north. The intention of the directional filtering is to isolate cutting noise from nearby vessel noise associated with a platform service ship, the *Harvey Challenger*. By isolating these sound sources, the contribution of conductor cutting noise to the power of LTSAs during conductor cutting activity was determined.

Next, the filtering method was applied to acoustic data gathered near a tidal energy converter, collected at Pacific Northwest National Laboratory’s Marine and Coastal Research Laboratory in the inlet of Sequim Bay, Washington State [Fig. 1(b)]. The target signal, mechanical noise from a small turbine on a gravity foundation, was around 20 dB less intense than the conductor cutting operations but propagated in a noisy tidal channel with regular boat traffic. The NoiseSpotter® was deployed 100 meters from the turbine at a bearing of 90° from February 1, 2024, through February 14, 2024, and recorded continuously during this time. The turbine operated during periods with strong currents through 11 February 2024. The direction of flood and ebb tides were roughly along the north-south axis.

The LTSA (Fig. 1) and azigrams were calculated for the entirety of both datasets. The directional display can also be used as a filter⁵—sound sources at distinct azimuths from a vector sensor can be isolated from one another in pressure spectrograms. Here, directional bins are identified based on the known location of a source of interest and used to construct a Boolean mask that is applied to the LTSA. The pressure spectrogram multiplied by this Boolean mask only contains time-frequency content from the chosen directional range.

The acoustic energy of the masked and unmasked spectrograms (units of dB re 1 μPa²/Hz) for each conductor cutting period were calculated by integrating acoustic pressure-squared over frequency and time according to

$$E = 10 \log_{10} \left(\int_{t_0}^{t_1} \int_{f_0}^{f_1} |p(t, f)|^2 df dt \right) \text{ dB re } 1 \mu\text{Pa}^2\text{s}, \tag{1}$$

where E is energy, p is acoustic pressure, t is time, t_0 and t_1 temporally bracket the window examined, f is frequency, f_0 and f_1 bracket the sensor’s frequency range. Time windows were identified as either the entirety of either a cutting period or tidal cycle.

3. Results

Instances of conductor cutting were reviewed, and the mechanical cutting of a single conductor pipe was selected as the subject of investigation due to the presence of vessel noise during two of three cutting periods. Vessel noise occurred for

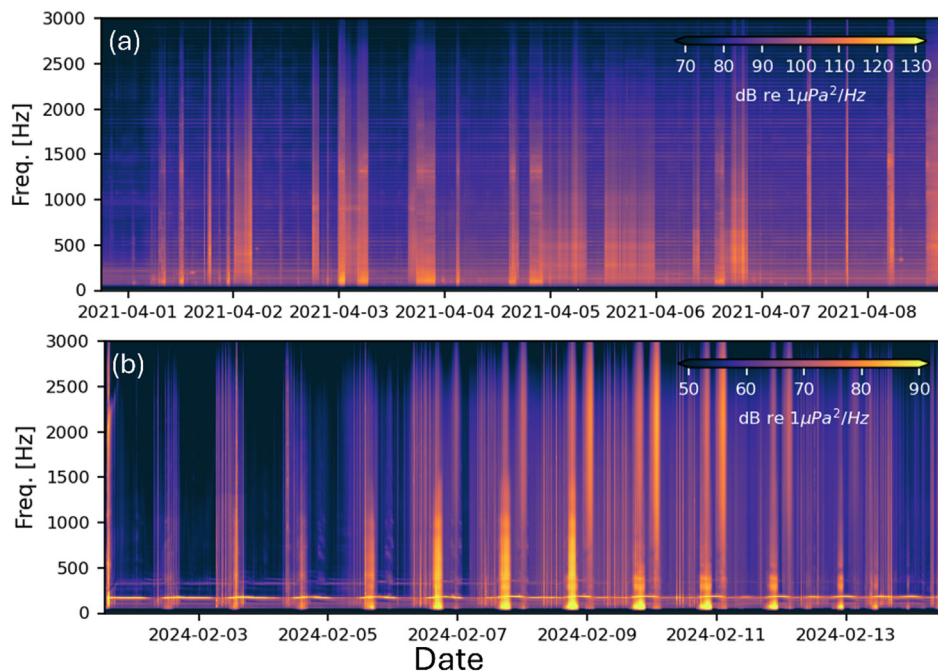


Fig. 1. LTSAs of (a) conductor cutting noise data collection period, and (b) tidal energy turbine data collection period.

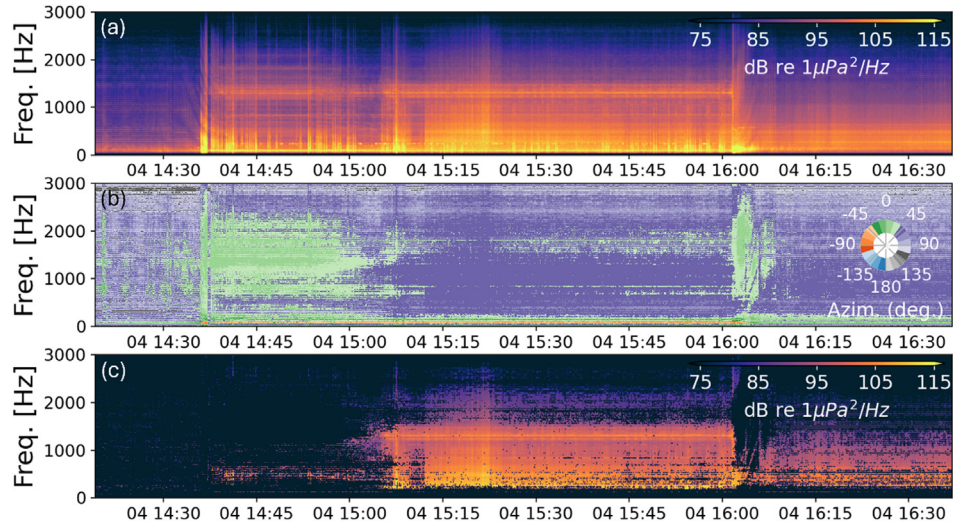


Fig. 2. (a) Unmasked spectrogram over a conductor cutting period 1 (April 4, 2021, 14:19–16:37), (b) azigram of conductor cutting period 1, (c) masked spectrogram of conductor cutting period 1, masked in a directional window from 40° to 60°.

only part of the first two conductor cutting periods. The service vessel was located near the eastern crane of the oil platform. The vessel’s distinct bearing to the vector sensor array from the conductor cut makes the two acoustic events distinguishable with the use of a directional filter. By isolating these two events, the contribution of vessel noise to measured acoustic energy was determined. Figure 2(c) shows a masked spectrogram between 40° and 60°—the approximate azimuthal range of the cutting activity for the mechanical cutting noise only. Notably, periods of vessel activity near 14:00 and 15:20 are missing once the mask is applied.

The tidal turbine dataset was filtered using the sequence of steps as was used on the Hermosa conductor cutting data, but for horizontal bearings between 75° and 115°, with a true bearing of the lander being 90°. The unmasked spectrogram, azigram, and masked spectrogram of one tidal cycle of turbine activity are shown in Fig. 3. The broadband streaks of energy at the beginning of the time window are known to be vessel noise [Fig. 3(a)] and are easily ignored by the directional filter. Other sounds, such as the signals in the 1500–3000 Hz frequency range (February 7, 16:30–19:00), and the period immediately after sounds from the northerly direction (February 7, 21:00–21:30) are just outside the directional window attributed to the tidal turbine. The application of the directional mask removes all but one of the vessel traffic noise occurrences from the spectrogram.

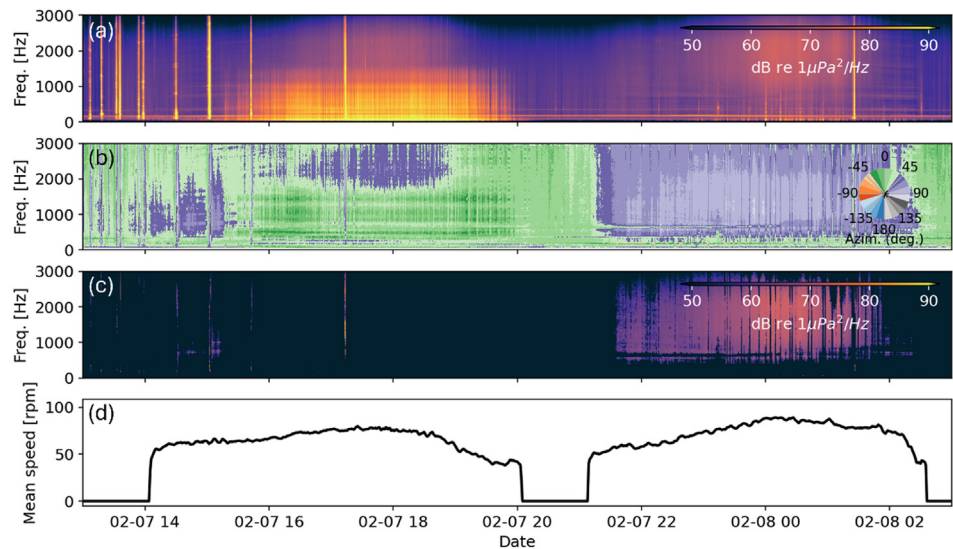


Fig. 3. (a) Unmasked spectrogram of tidal turbine over one tidal cycle (07 Feb 2024 12:00 to 08 Feb 2024 02:00) in Sequim Bay, WA, (b) azigram over the tidal cycle, (c) masked spectrogram over the tidal cycle, mased over 75° to 115°, (d) rotations per minute (rpm) of tidal turbine during flood tide, followed by ebb tide, for the same tidal cycle.

Table 1. Unfiltered and directionally filtered energy for each conductor cutting period examined (dB re 1 $\mu\text{Pa}^2 \text{ s}$).

	Period 1	Period 2	Period 3
Unfiltered	173 dB	180.15 dB	170.56 dB
Filtered	166.52 dB	175.65 dB	168.70 dB
Difference	-6.46 dB	-4.5 dB	-1.85 dB

It is also observed in Fig. 3 that no tidal turbine sounds are observed during the flood tide. This is possibly due to somewhat lower turbine rotation rates during the flood tide relative to the ebb tide or the turbine configuration itself. This effect was intermittently observed throughout the data set [Figs. 1(c) and 1(d)]. A deeper evaluation of why this phenomenon is observed is beyond the scope of this letter.

Next, an example of mechanical cutting contributions in terms of acoustic energies [calculated by using the masked and unmasked spectrograms from Figs. 2 and 3 in Eq. (1)] for each conductor cutting period is summarized in Table 1. The difference between the unmasked and masked spectrogram energies indicates a 4.5–6.5 dB contribution of vessel noise to the overall acoustic energy during each event.

Mean frequency spectra were computed over the unmasked and masked time periods for cutting period 1 (oil platform) and one tidal cycle (tidal turbine). A distinct difference is seen (Fig. 4) when data are selected based on directional bins, with the key result being lower energy levels and spectral shape for the directionally filtered spectrum vs the unfiltered spectrum. For example, for the conductor cutting example, much of the lower frequency content below 300 Hz that comes from a different direction in Fig. 3 is not attributed to the spectrum associated with conductor cutting. Directional filtering of tidal turbine sounds is seen to highlight the tonal structure of radiated sound while helping suppress some of the broadband ambient noise from outside the directional window.

4. Conclusions

A directional filtering method was demonstrated for two marine energy applications using azigrams to parse data into directional bins. The omnidirectional spectrograms, when filtered by the directional azigrams, yield insight into the specific contributions of an acoustic source being characterized. As a result of directional filtering, omnidirectional spectra for both case studies are seen to have more energy than the filtered spectra, but also a somewhat different shape and frequency content. Like differences in directionally filtered and unfiltered spectra, total average energy is also lower for the directionally filtered case relative to the unfiltered case. Of course, the way filtered power calculations include or exclude acoustic data outside the directional window of interest should change the way these calculations are interpreted.

In terms of implications for SSV, the directionally filtered spectra, when backpropagated to estimate the source spectra, can result in a different (potentially more representative) modeled field for a specific sound source. Consequently, more precise energies, dosage levels, and spectra can be attributed to specific sources of sound. With further exploration of these techniques, more accurate and thorough SSV is possible.

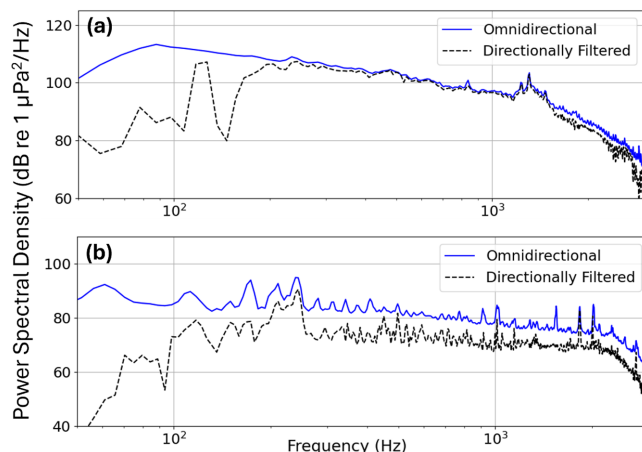


Fig. 4. (a) Frequency spectra of conductor cutting period 1 (April 4, 2021 14:19 to 16:37) calculated from unfiltered and directionally filtered power spectral averages, (b) frequency spectra of tidal turbine operation throughout one tidal cycle (from 12:00 February 7, 2024, to 02:00 February 8, 2024) in Sequim Bay, WA.

Acknowledgments

Study concept, oversight, and funding were provided by the U.S. Department of the Interior, Bureau of Ocean Energy Management, Environmental Studies Program, Washington, DC, under Contract No. 140M0120C0011 to TetraTech.

Author Declarations

Conflict of Interest

The authors have no conflicts to disclose.

Data Availability

The data that support the findings of this study are available from the corresponding author upon reasonable request.

References

- ¹R. Racca, M. Austin, A. Rutenko, and K. Bröker, "Monitoring the gray whale sound exposure mitigation zone and estimating acoustic transmission during a 4-D seismic survey, Sakhalin Island, Russia," *Endang. Species Res.* **29**(2), 131–146 (2015).
- ²R. Wyatt, "Review of existing data on underwater sound produced by the oil and gas industry" (Seiche Ltd., Devon, UK, 2008).
- ³A. Thode, J. Skinner, P. Scott, J. Roswell, J. Straley, and K. Folkert, "Tracking sperm whales with a towed acoustic vector sensor," *J. Acoust. Soc. Am.* **128**(5), 2681–2694 (2010).
- ⁴A. M. Thode, T. Sakai, J. Michalec, S. Rankin, M. S. Soldevilla, B. Martin, and K. H. Kim, "Displaying bioacoustic directional information from sonobuoys using azigrams," *J. Acoust. Soc. Am.* **146**(1), 95–102 (2019).
- ⁵L. Tenorio-Hallé, A. M. Thode, M. O. Lammers, A. S. Conrad, and K. H. Kim, "Multi-target 2D tracking method for singing humpback whales using vector sensors," *J. Acoust. Soc. Am.* **151**(1), 126–137 (2022).
- ⁶K. Raghukumar, G. Chang, F. Spada, and C. Jones, "A vector sensor-based acoustic characterization system for marine renewable energy," *J. Mech. Sci. Eng.* **8**(3), 187 (2020).
- ⁷R. D. McCauley, "Measurement of underwater noise produced during wellhead cutting operations and an estimation of its environmental influence. Centre for marine science and technology report," CMST Report No. 2003-20 (Curtin University, Perth, Australia, 2004).
- ⁸T. Pangerc, S. Robinson, P. Theobald, and L. Galley, "Underwater sound measurement data during diamond wire cutting: First description of radiated noise," *Proc. Mtgs. Acoust.* **27**(1), 040012 (2016).
- ⁹Freibott, A. (2024). "First tidal turbine in the Pacific Northwest signals wave of the future," available at <https://www.pnnl.gov/publications/first-tidal-turbine-pacific-northwest-signals-wave-future> (Last viewed February 5, 2025).
- ¹⁰S. M. Wiggins and J. A. Hildebrand, "High-frequency acoustic recording package (HARP) for broad-band, long-term marine mammal monitoring," in *Proceedings of the 2007 Symposium on Underwater Technology and Workshop on Scientific Use of Submarine Cables and Related Technologies*, Tokyo, Japan (April 17–20, 2007), pp. 551–557.